

## Article

# Kinetic Control of Aqueous Polymerization Using Radicals Generated in Different Spin States

Ignacio Rintoul

Consejo Nacional de Investigaciones Científicas y Técnicas, Universidad Nacional del Litoral,  
Santa Fe 3000, Argentina; irintoul@santafe-conicet.gov.ar; Tel.: +54-342-451-1370

Academic Editor: Alexander Penlidis

Received: 3 January 2017; Accepted: 17 March 2017; Published: 24 March 2017

**Abstract:** Background: Magnetic fields can interact with liquid matter in a homogeneous and instantaneous way, without physical contact, independently of its temperature, pressure, and agitation degree, and without modifying recipes nor heat and mass transfer conditions. In addition, magnetic fields may affect the mechanisms of generation and termination of free radicals. This paper is devoted to the elucidation of the appropriate conditions needed to develop magnetic field effects for controlling the kinetics of polymerization of water soluble monomers. Methods: Thermal- and photochemically-initiated polymerizations were investigated at different initiator and monomer concentrations, temperatures, viscosities, and magnetic field intensities. Results: Significant magnetic field impact on the polymerization kinetics was only observed in photochemically-initiated polymerizations carried out in viscous media and performed at relatively low magnetic field intensity. Magnetic field effects were absent in polymerizations in low viscosity media and thermally-initiated polymerizations performed at low and high magnetic field intensities. The effects were explained in terms of the radical pair mechanism for intersystem crossing of spin states. Conclusion: Polymerization kinetics of water soluble monomers can be potentially controlled using magnetic fields only under very specific reaction conditions.

**Keywords:** magnetic field; radical polymerization; quantum chemistry; acrylamide; solution polymerization; photopolymerization; process control

## 1. Introduction

Magnetic field (MF) effects in chemical kinetics have a long tradition. Early in 1929 Bhatnagar observed that the rate of decomposition of hydrogen peroxide is influenced by MF [1]. Afterwards, in 1946, Selwood observed that the efficiency of some catalyst can be increased in the presence of MF [2]. These early works gave birth to the fascinating idea of controlling chemical reactions using MF. The discovery and understanding of nuclear and electronic spin polarization phenomena during chemical reactions in the late 1960s contributed significantly to the development of this idea. Up to now, MF effects in chemical reactions have been observed in a number of situations and have received proper theoretical analysis. However, MF effects in free radical polymerizations has not yet found a practical application [3].

Table 1 summarizes several MF effects observed in polymerization studies. MF effects reveal the possibility to control the kinetics of radical polymerizations and the chain architecture of resulting polymers in a homogeneous, instantaneous, and highly selective way. In addition, MF effects in polymerization reactions can be carried out without physical contact, independently of the temperature, pressure, and agitation degree of the reacting medium, and without modifying recipe formulations, heat and mass transfer conditions, nor any other reaction parameter normally used to control the course of polymerization.

**Table 1.** Summary of MF effects on radical polymerization reported in the literature.

Monomer	Initiator	System	MF Effect	Ref.
AN	AIBN	Bulk	Increase of $R_p$ , polymer yield, molar mass, syndiotacticity, crystallinity, and thermal stability of resulting polymers	[4]
MMA, ST	AIBN	Bulk	No effect	[4]
MMA	MB	H <sub>2</sub> O-MeOH mixtures	Decrease of the polymer yield and increase of the molar mass polymers	[5]
MMA	MB	Aqueous solution	No effect	[5]
MMA	BP, AMP, APA, AHC	Aqueous solution	Increase of the initiator efficiency and decrease of the monomer exponent and molar mass	[6]
AC, MMA, AM	BP, AMP, APA, AHC	Several solvents	Increase of the initiator efficiency and thermal stability of polymers	[7]
MMA, EMA, BMA	AIBN	Bulk	Increase of molar mass and thermal stability of products	[8]
ST	AIBN	H <sub>2</sub> O-EG mixtures	Increase of molar mass and homogeneity of polymers	[9]
MMA, ST	BP	Liquid CO <sub>2</sub>	Increase of conversion and molar mass	[10]
MMA, ST	BP	Cyclohexane	No effect	[10]
MMA, EMA, BMA	BP	Bulk	Increase of $R_p$ and molar mass	[11]
ST	BK	Emulsion	Increase of $R_p$ and molar mass	[12,13]
ST, MMA, AA	BK	Emulsion	Increase of $R_p$ and molar mass	[14]
ST, MMA	AIBN	Emulsion	Increase of molar mass and decrease of molar mass distribution	[15]
ST	K <sub>2</sub> S <sub>2</sub> O <sub>8</sub>	Emulsion	Decrease of $R_p$	[16]
MMA	BP	10 different organic solvents	Increase of $R_p$ and conversion and decrease of the induction period for initiation	[17]
MMA	TX	Dimethylformamide	Increase of conversion and molar mass	[18]
AM	MB	H <sub>2</sub> O-EG mixtures	Increase of $R_p$	[19]
AM, AA, DADMAC and combinations	C <sub>26</sub> H <sub>27</sub> O <sub>3</sub> P	H <sub>2</sub> O-EG mixtures	Increase of $R_p$ of all monomers in homo and copolymerizations. Increase of molar mass of polyAA. No effect in the molar mass of polyAM and copolymer compositions	[20,21]

AA: acrylic acid, AC: vinyl acetate, AHC: 1,1'-azobis(cyclohexane-1-carbonitrile); AIBN: 2,2'-azobisisobutyronitrile; AM: acrylamide, AMP: 2,2'-azobis(2-methylpropionitrile); AN: acrylonitrile; APA: 4,4'-azobis(4-cyanopentanoic acid); BK: benzyl ketone; BMA: butylmethacrylate; BP: benzoyl peroxide, C<sub>26</sub>H<sub>27</sub>O<sub>3</sub>P: phenyl-bis(2,4,6-trimethylbenzoyl)-phosphine oxide; DADMAC: diallyldimethylammonium chloride; EMA: ethylmethacrylate, K<sub>2</sub>S<sub>2</sub>O<sub>8</sub>: potassium persulfate; MB: methylene blue; MMA: methylmethacrylate; ST: styrene; TX: thioxanthone.

The aim of this work is to establish some criteria for recipe preparation and reaction conditions needed to study the MF effects on the kinetics of radical polymerization of acrylamide (AM) [22] and to conclude the consequences for the overall rate expression expressed as Equation (1) and the kinetic chain length expressed as Equation (2) [23]:

$$R_p = k_p \cdot [M]^a \cdot \left( \frac{f \cdot k_d \cdot [I]}{k_t} \right)^\beta \quad (1)$$

$$\nu = \frac{k_p \cdot [M]}{2 \cdot (f \cdot k_d \cdot k_t \cdot [I])^{0.5}} \quad (2)$$

Here  $R_p$  is the polymerization rate defined as the negative derivative of the monomer concentration with time.  $[M]^a$  and  $[I]^\beta$  are the monomer and initiator concentrations in mol/L powered to their respective reaction orders,  $k_p$  and  $k_t$  are the propagation and termination rate coefficients in L/mol·s, and  $f$  and  $k_d$  are the efficiency and decomposition rate of the initiator. In photopolymerization reactions,  $f$  is called the quantum yield of the photoinitiator,  $\Phi$  and  $k_d$  is expressed according to Equation (3):

$$k_d = \varepsilon \cdot I_0 \quad (3)$$

Here  $\varepsilon$  is the molar absorptivity of the photoinitiator, in L/mol·cm, and  $I_0$  is the light intensity in the polymerization medium in mol/L·s.

Full theoretical description of the interaction between MF and reactants is not the task of this work since it can be consulted in the excellent review paper of Steiner and Ulrich [24]. In any case, a short overview of the fundamentals of three interesting MF phenomena commonly hypothesized as explanations for MF effects in polymerization reactions is presented.

Thermal equilibrium of spin states act at the electron level. This suggests that chemical reactions should be accelerated by magnetically-induced diamagnetic/paramagnetic transitions in the reactive species. If  $N$  spins are present in a polymerization medium under a steady MF of intensity  $B_0$ ,  $N_\alpha$ , and  $N_\beta$  spins will be magnetic moment spin up,  $m_s = 0.5$ , and down,  $m_s = -0.5$ , respectively. The conservation law of the total spin value establishes that:  $N = N_\alpha + N_\beta$  and the ratio between  $N_\alpha$  and  $N_\beta$  is given by Equation (4) [25]:

$$\frac{N_\alpha}{N_\beta} = e^{\frac{g \cdot \beta \cdot B_0}{k \cdot T}} \quad (4)$$

Here  $g$  is the electron “ $g$ ” factor,  $\beta$  is the electronic Bohr magneton,  $\beta = 0.92731 \times 10^{-20}$  erg/gauss,  $k$  is the Boltzmann constant,  $k = 1.38044 \times 10^{-16}$  erg/K, and  $T$  is the temperature of the system [25]. Under normal conditions where free radical reactions are carried out immersed in the geomagnetic field (~0.5 Gauss), the ratio  $N_\alpha/N_\beta$  is very close to unity and consequently equal populations of spins up and down can be assumed. Thermodynamically, the magnetic contribution to the free enthalpy of the reaction,  $\Delta G_m$ , in an externally-applied MF of intensity  $B_0$  can be expressed as Equation (5) [24]:

$$\Delta G_m = -\frac{1}{2} \cdot \Delta \chi_M \cdot B_0^2 \quad (5)$$

Here  $\Delta \chi_M$  is the change of the magnetic susceptibility during the reaction of one molar unit. Therefore, according to Equations (4) and (5), the higher the MF intensities and the lower the temperatures are, the more important the MF effects on  $f$  and  $k_t$  will be.

MF-induced molecular orientation acts at the molecule level. MF tends to align molecules that present magnetic susceptibility,  $\Delta \chi_M \neq 0$ . Conversely, temperature tends to randomize the orientation of molecules. Therefore, an average orientation results from the balance between these two opposed effects. Classically, the energy of a molecular dipole oriented with a  $\theta$  angle to a MF is given by Equation (6) [26]. Equation (7) is the

Boltzmann form of the average orientation of molecular dipoles,  $P(\theta)$ , as a function of the MF intensity, the temperature of the system and  $\Delta\chi_M$  of the molecules:

$$E = \Delta\chi_M \cdot B \cdot \cos(\theta) \quad (6)$$

$$P(q) = \frac{e^{\left(\frac{Dc_m \cdot B \cdot \cos(q)}{R \cdot T}\right)}}{\int_0^{2\pi} e^{\frac{Dc_m \cdot B \cdot \cos(q)}{R \cdot T}} dq} \quad (7)$$

Here  $P(\theta)$  is the normalized probability to find the molecule oriented with an angle  $\theta$  to the direction of an effective MF of magnitude  $B$ .  $B$  is defined according to Equation (8):

$$B = B_0 + B_c \quad (8)$$

Here  $B_c$  is the resulting magnetic contribution due to the  $B_0$  induced alignment of all molecules. Evidently, it is expected a certain influence of molecular orientation of monomers and growing radicals on  $k_p$  and  $k_t$ .

The radical pair mechanism for spin states acts at the supramolecular level. Initiator molecules are hypothesized to exist in cages formed by solvent and monomer molecules. Eventually, a molecular initiator can decompose, generating a caged radical pair. Caged radical pairs are generated in singlet ( $S$ ) or triplet ( $T_+$ ,  $T_0$ ,  $T_-$ ) spin states from precursors having their respective multiplicity, or when formed by free radical encounters. These spin states describe different electron configurations. Depending on these configurations the caged radical pair may recombine regenerating the initial molecule, undergoing the formation of cage products which generates a new molecule, or the radicals can escape from the cage releasing two free radicals to the reaction medium. Radical pairs in the  $S$  state have extremely high probability to undergo recombination reactions and/or formation of cage products. Conversely, radical pairs in any of the three  $T$  states cannot recombine. Nevertheless, radicals may pass from one state to another through intersystem crossing mechanisms. The energy associated with the  $T_+$  and  $T_-$  states increases and decreases proportionally with the MF intensity, while the energy of the  $S$  and  $T_0$  states are unaffected by the MF. The application of MF splits out the energy levels of the  $T$  states diminishing substantially the probability for intersystem crossing to the  $S$  state. Therefore, primary caged radical pairs can be quenched in the  $T$  state, decreasing the probability of radical recombination. Consequently, more radicals are released to the polymerization medium resulting in an increase of the initiator efficiency leading to an increase of  $R_p$ . The MF-induced modification of the outcome of caged radical pairs is eventually interpreted as an MF-induced change of  $\Phi$  or  $f$ . Furthermore, when two growing radicals encounter each other in the  $T$  state, they cannot recombine. This effect is interpreted as a decrease of  $k_t$ . Thus, the radicals continue growing increasing  $v$ .

Finally,  $[M]$ ,  $[I]$ ,  $\alpha$ , and  $\beta$  are not affected by any MF mechanism.

## 2. Materials and Methods

### 2.1. Materials

Ultra-pure AM, four times recrystallized, (AppliChem, Darmstadt, Switzerland) was selected as the monomer. An aqueous dispersion of  $C_{26}H_{27}O_3P$ , (Ciba Specialty Chemicals, Basel, Switzerland) and potassium persulfate,  $K_2S_2O_8$ , (Fluka Chemie, Buchs, Switzerland) served as photo- and thermal-initiators. Photochemical decomposition of  $C_{26}H_{27}O_3P$  and thermal decomposition of  $K_2S_2O_8$  generate radical pairs in triplet and singlet spin states, respectively. [27] The water was of Millipore quality (18.2 M $\Omega$ -cm). Ethylene glycol 99% for synthesis (EG) (AppliChem, Darmstadt, Switzerland) was used to vary the viscosity of the polymerization medium. Acetonitrile for high performance liquid chromatography (HPLC) (AppliChem, Darmstadt, Switzerland) served to precipitate the polymer in the withdrawn samples.

## 2.2. Polymer Synthesis

Syntheses were performed in a 100 mL glass reactor (3 cm diameter, 15 cm height) equipped with a UV lamp, stirrer, condenser, gas inlet, and a heating/cooling jacket. The UV lamp had a primary output at 254 nm wavelength with constant and uniform irradiation everywhere in the reaction medium,  $I_0 = 5.16 \times 10^{-8}$  mol/L·s. The same reactor, without the UV lamp, was used for thermally-initiated polymerizations. The reactor was entirely placed between the poles of an electromagnet (Bruker-EPRM, Rheinstetten, Germany) for polymerizations carried out in the range  $0 < MF < 0.5$  Tesla and in the core of a superconductor magnet (Bruker-UltraShield, Rheinstetten, Germany) for polymerizations carried out in the range  $0.5 < MF < 7$  Tesla. A thermostat adjusted the reaction temperature within  $\pm 1$  K. Oxygen was removed from the initial monomer solution by purging with  $N_2$  ( $O_2 < 2$  ppm; Airliquide, Gümligen, Switzerland) during 30 min at 273 K and 0 Tesla of MF intensity. After degassing, the temperature was raised to activate the decomposition of  $K_2S_2O_8$  in case of thermally initiated polymerization and the UV lamp was lighted to activate the photodecomposition of  $C_{26}H_{27}O_3P$  in case of photopolymerization. Simultaneously, the MF was adjusted to the specified intensity. Complementary experiments were carried out for comparison, without MF, though keeping constant all the other conditions. All reactions were performed isothermally during 60 min continuous purging with  $N_2$  and drawing samples of 0.1–0.2 g from the reactor every 5 min for kinetic analysis. Table 2 summarizes the conditions of all polymerizations.

**Table 2.** Summary of polymerization conditions.

Series	MF Tesla	[AM] mol/L	[Initiator] mol/L	Solvent	Temp. K
1	0.0	0.20	-	H <sub>2</sub> O	313
2	0.0	0.20	$[C_{26}H_{27}O_3P] = 2 \times 10^{-6}$	H <sub>2</sub> O	323
3	0.0	0.20	$[K_2S_2O_8] = 2.3 \times 10^{-3}$	H <sub>2</sub> O	273
4	0.0 7.0	0.15	$[K_2S_2O_8] = 2.3 \times 10^{-3}$	H <sub>2</sub> O	308
5	0.0 7.0	0.15	$[K_2S_2O_8] = 2.3 \times 10^{-3}$	50% EG	308
6	$7.0 < MF < 0.5$	0.10	$[K_2S_2O_8] = 2.3 \times 10^{-3}$	H <sub>2</sub> O	308
7	0.00 0.11 0.35 0.50	0.20	$[K_2S_2O_8] = 1.2 \times 10^{-2}$	H <sub>2</sub> O	313
8A 8B	$0.0 < MF < 0.5$	0.20 0.10	$[K_2S_2O_8] = 1.2 \times 10^{-2}$	H <sub>2</sub> O	313
	$0.0 < MF < 0.1$		$[K_2S_2O_8] = 1.2 \times 10^{-3}$		
9	0.0 0.1	0.20	$[C_{26}H_{27}O_3P] = 1 \times 10^{-6}$	H <sub>2</sub> O	313
10	0.0 0.1	0.20	$[C_{26}H_{27}O_3P] = 1 \times 10^{-6}$	50% EG	313

The first three series were performed to demonstrate the absence of side radical generation which could disturb the polymerization path. An initiator-free aqueous AM solution was illuminated with UV light during one hour at 313 K to verify the absence of monomer photolysis (series 1). Another AM solution containing  $C_{26}H_{27}O_3P$  was maintained in darkness during one hour at 323 K to demonstrate the absence of thermal decomposition of the photoinitiator (series 2). Finally, AM- $K_2S_2O_8$  was maintained for 1 h at 273 K to prove the absence of  $K_2S_2O_8$  decomposition during degassing (series 3).  $K_2S_2O_8$  was used within the limiting reaction conditions suitable for radical generation through the monomer-enhanced mechanism [28].

Series 4–9 represent the main experiments. Recipe formulations and reaction conditions without magnetic fields were adjusted to obtain linear conversion curves. Linear conversion paths facilitate the data analysis. Series 4 and 5 were designed to evaluate the effects of 7 Tesla MF intensity in polymerizations initiated with radicals in singlet spin state (i.e., thermally-initiated polymerizations) performed in aqueous monomer solution of relatively low viscosity,  $\eta = 1.03 \times 10^{-3}$  Pa·s and in 50 wt% of EG aqueous monomer solution with relatively high viscosity,  $\eta = 5.16 \times 10^{-3}$  Pa·s. Series 6–8 were designed to evaluate the effect of MF varying continuously from 7 Tesla to 0.5 Tesla, four MF intensities between 0 and 0.5 Tesla and MF varying continuously from 0 to 0.5 Tesla (series 8A) and from 0 to 0.1 Tesla (series 8B) in polymerizations initiated with radicals in singlet spin state (i.e., thermally-initiated polymerizations) using water as a solvent, respectively. Series 9 and 10 were designed to evaluate the effect of 0.1 Tesla MF intensity in polymerizations initiated with radicals in triplet spin state (i.e., photochemically-initiated polymerizations) using water,  $\eta = 1.09 \times 10^{-3}$  Pa·s and 50 wt % EG aqueous solution,  $\eta = 5.20 \times 10^{-3}$  Pa·s as solvents, respectively.

### 2.3. Analytics and Instruments Calibration

The dynamic viscosity,  $\eta$ , of monomer aqueous solutions and monomer solutions with 50 wt % EG was measured at their specified reaction temperatures using a disc viscometer (Brookfield, Middleboro, USA) equipped with a 250 mL thermostatted ( $\pm 1$  K) vessel and a disc spindle of 20 mm diameter rotating at 50 rpm. The viscosity of each monomer solution was measured five times. Deviations were within 4%.

The conversion was determined analyzing the residual monomer concentration. It served to calculate  $R_p$  and  $v$  according to a detailed procedure [29]. Briefly, the residual monomer concentration in the samples was monitored using a HPLC system composed of an L-7110 Merck-Hitachi pump (Hitachi, Tokyo, Japan) and a SP6 Gynkotek UV detector (Gynkotek, Germering, Germany) operating at  $\lambda = 197$  nm. The stationary and mobile phases were LiChrosphere 100 RP-18 (Merck, Darmstadt, Germany) and aqueous solutions containing 5 wt% acetonitrile. The flow rate was 1 mL/min. The HPLC system was calibrated using AM solutions of known concentrations. The concentration as a function of the peak area served as calibration parameter ( $r^2 > 0.999$ ). Figure 1 presents the calibration curve of the HPLC system. The samples were mixed with 4 mL of acetonitrile to precipitate and isolate the polymer from the solution. The non-reacted monomers remained in solution. 20  $\mu$ L of the supernatant were injected for HPLC analysis.

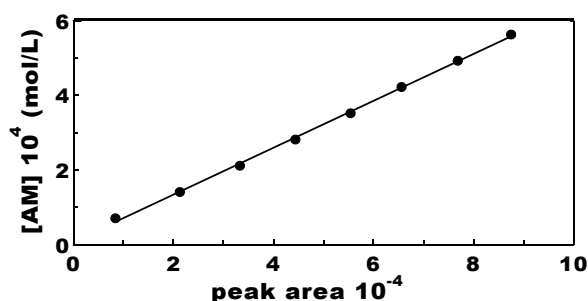


**Figure 1.** HPLC calibration curve. The concentration of standard AM solutions were plotted as a function of the corresponding peak areas.  $r^2 > 0.999$ .

Due to the limited space between the poles of the electromagnet and in the superconductor bore, it was not possible to simultaneously install both probes to measure the MF and the polymerization reactor there. Consequently, the MF was known indirectly. Probes were installed between the poles of the electromagnet in order to measure the MF for different electrical currents running through the bobbins of the magnet. With such information the calibration curve, MF strength vs. electrical current was determined. The magnetic probes were moved from the gap between the poles and the reactor was installed. The MF was adjusted by setting the electrical current according to the calibration curve presented in Figure 2.

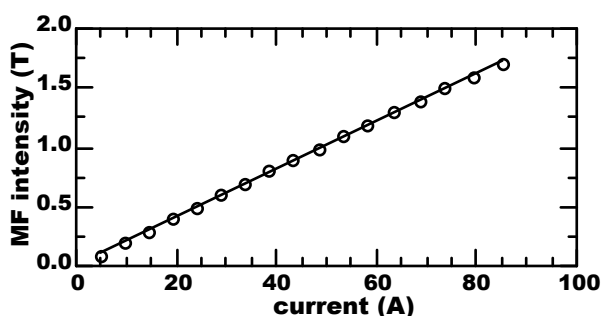


**Figure 2.** Electromagnet calibration. Magnetic field (MF) strength vs. electrical current (Amperes),  $r^2 > 0.999$ .

In case of polymerizations carried out in the superconductor magnet, the MF intensity was varied moving the reactor along the magnet bore. A magnetic probe was placed at different distances from the top of the

magnet in order to determine the calibration curve shown in Figure 3. The MF was adjusted by setting the distance between the reactor and the core of the magnet according to the calibration curve.

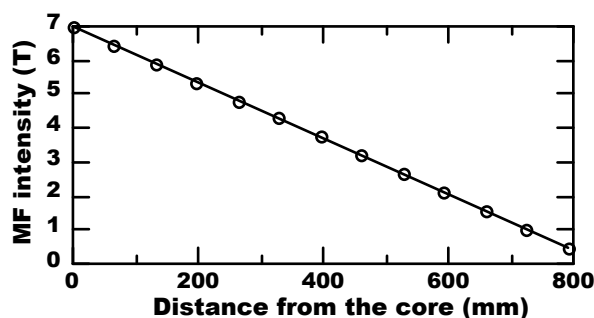
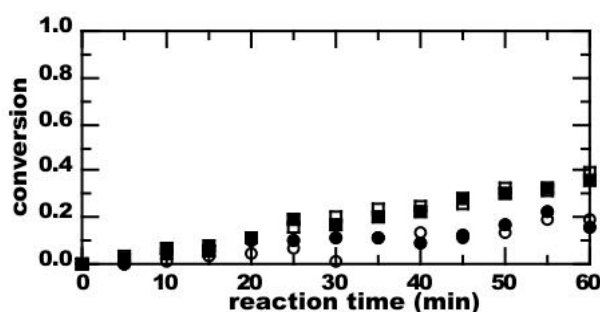


**Figure 3.** Superconductor magnet calibration. Magnetic field (MF) strength vs. distance from the core,  $r^2 > 0.999$ . The origin was defined at the highest MF intensity (7 Tesla) in the middle of the magnet.

### 3. Results

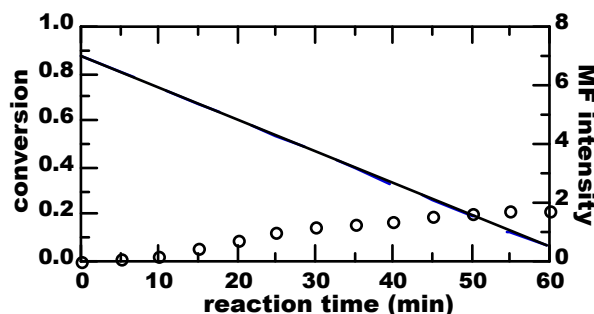
The absence of polymerization was confirmed for series 1–3 demonstrating that the polymerization path was not disturbed by side radical generation.

Figure 4 shows that thermally-initiated polymerizations carried out at 7 Tesla progressed identically to those performed without MF. However, polymerizations carried out using 50 wt % EG aqueous solution as solvent progressed faster than those performed using pure water as solvent.



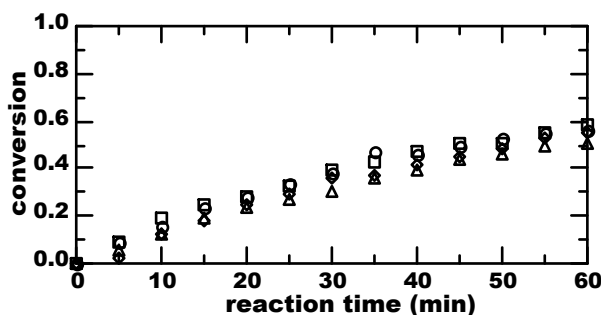
**Figure 4.** Conversion of AM vs. reaction time for polymerizations carried out using water, series 4 (●) and 50 wt % EG aqueous solution, series 5 (■), as solvents. MF intensity: 7 Tesla (full symbols), without MF (empty symbols). [AM] = 0.15 mol/L,  $[K_2S_2O_8] = 2.3 \times 10^{-3}$  mol/L,  $T = 308$  K.

Figure 5 shows that thermally-initiated polymerizations using water as solvent still progressed linearly in spite of the fact that the MF intensity varied from 7 to 0.5 Tesla during the 60 min of reaction time.



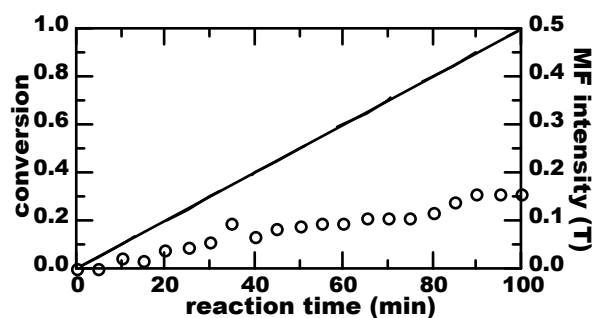
**Figure 5.** Conversion of AM (○) vs. reaction time. The MF intensity (—) varied from 7 Tesla at the beginning of polymerization to 0.5 Tesla after 60 min of reaction. Series 6. [AM] = 0.10 mol/L,  $[K_2S_2O_8] = 2.3 \times 10^{-3}$  mol/L,  $T = 308$  K, solvent: water.

Figure 6 shows no substantial differences between thermally-initiated polymerizations using water as solvent when carried out at 0.00, 0.11, 0.35, and 0.50 Tesla.



**Figure 6.** Conversion of AM vs. reaction time for polymerizations carried out at different MF intensities. MF = 0 ( $\circ$ ), 0.11 ( $\square$ ), 0.35 ( $\diamond$ ), 0.50 ( $\Delta$ ) Tesla. Series 7.  $[AM] = 0.20$  mol/L,  $[K_2S_2O_8] = 1.2 \times 10^{-2}$  mol/L,  $T = 313$  K, solvent: water.

Figures 7 and 8 show that thermally-initiated polymerizations using water as solvent were not accelerated, nor slowed by any MF intensity in the ranges 0 to 0.5 and 0 to 0.1 Tesla, respectively.



**Figure 7.** Conversion of AM ( $\circ$ ) vs. reaction time. The MF intensity (—) varied from 0 Tesla at the beginning of polymerization to 0.5 Tesla after 100 min of reaction. Series 8A.  $[AM] = 0.20$  mol/L,  $[K_2S_2O_8] = 1.2 \times 10^{-2}$  mol/L,  $T = 313$  K, solvent: water.

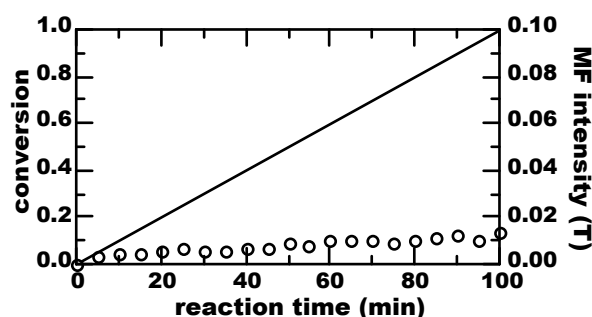


**Figure 8.** Conversion of AM ( $\circ$ ) vs. reaction time. The MF intensity (—) varied from 0 Tesla at the beginning of polymerization to 0.1 Tesla after 100 min of reaction. Series 8B.  $[AM] = 0.10$  mol/L,  $[K_2S_2O_8] = 1.2 \times 10^{-3}$  mol/L,  $T = 313$  K, solvent: water.

Figure 9 shows that aqueous photopolymerizations carried out at 0.1 Tesla of MF intensity progressed slightly faster than aqueous photopolymerizations carried out without MF.



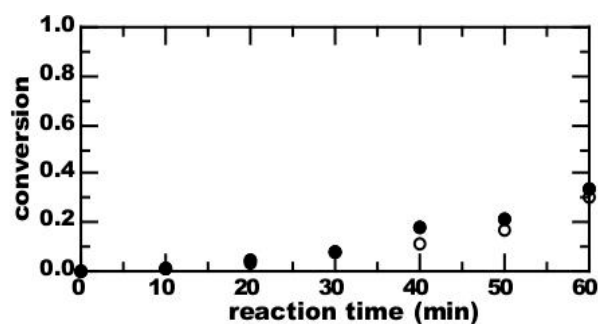


**Figure 9.** Conversion of AM vs. reaction time for polymerizations carried out at 0.1 Tesla of MF intensity (●) and without MF (○). Series 9.  $[AM] = 0.20$  mol/L,  $[C_{26}H_{27}O_3P] = 1 \times 10^{-6}$  mol/L,  $T = 313$  K, solvent: water.

Figure 10 shows that the effect of 0.1 Tesla on photopolymerizations was significantly enhanced when the reaction is carried out in a medium with higher viscosity.

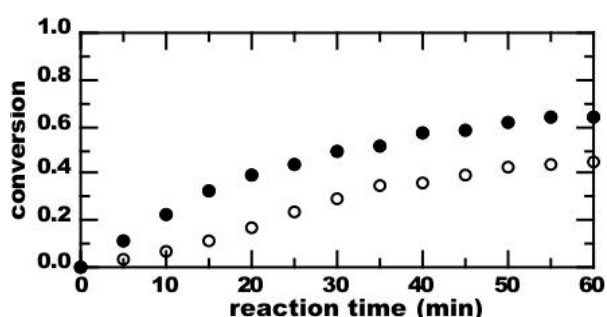


**Figure 10.** Conversion of AM vs. reaction time for polymerizations carried out at 0.1 Tesla of MF intensity (●) and without MF (○). Series 10.  $[AM] = 0.20$  mol/L,  $[C_{26}H_{27}O_3P] = 1 \times 10^{-6}$  mol/L,  $T = 313$  K, solvent: 50 wt % EG in water.

## 4. Discussion

Variations of at least 20% in the value of  $R_p$  in reference to the  $R_p$  value without MF were considered to evaluate the presence or absence of MF effects.

### 4.1. Thermal Equilibrium of Spin States

Assuming free electrons in the empty space, the ratio  $N_\alpha/N_\beta$  can be calculated as 1.03 and 1.0004 at 7 Tesla and 0.1 Tesla, respectively. Such small differences in the population of  $N_\alpha$  and  $N_\beta$  can hardly be detected since they are within the range of experimental error. However, it is important to note that uncoupled electrons in radical species occurring in polymerization systems are far from being free electrons in the empty space. In any case, the identical polymerization paths of reactions carried out with and without MF observed in Figure 4 (series 4 and 5) and the linear progression of polymerization in Figure 5 (series 6) prove that changes in the thermal equilibrium of spin states due to high MF intensity interactions over uncoupled electrons is insignificant. Any MF effect would be manifested as a change in the slope of the conversion-time plot. As conversion evolved linearly (constant slope) in spite of the fact MF varied, no MF effect could be evidenced when applied in this reaction condition and thus, no MF induced changes can be assigned to  $f$  and  $k_t$ .

### 4.2. Magnetically-Induced Molecular Orientation

$\Delta\chi_M$  for AM, H<sub>2</sub>O and EG, the main components of the polymerization medium, are reported as  $-2.3 \times 10^{-3}$ ,  $-1.6 \times 10^{-3}$ , and  $-2.6 \times 10^{-3}$  mL/mol, respectively [30]. Introducing the values of  $\Delta\chi_M$  into Equation (5), the relative orientation of AM, H<sub>2</sub>O, and EG molecules under the conditions specified for series 4 were determined and presented in Figure 11. Evidently, the contribution of 7 Tesla of MF intensity to the orientation of either AM, H<sub>2</sub>O, and EG is minimal. Specifically, the probability to find an AM molecule oriented in the

direction of MF is only 1.3% higher than perpendicular,  $\pi/2$ -radians, to the field. For water and EG it resulted 0.9 and 2%, respectively. Evidently, these small orientations resulted in insignificantly modifying the polymerization rate of AM as it was observed in Figures 4 to 9 (series 4–9). Therefore, no MF-induced changes can be assigned to  $k_p$  and  $k_t$ .

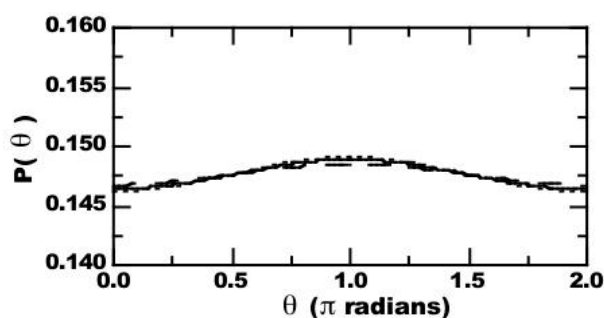


**Figure 11.** Magnetically-induced orientation of AM (—), H<sub>2</sub>O (---), and EG (···) at 7 Tesla of MF strength and 308 K.

#### 4.3. Radical Pair Mechanism

The polymerization rate increased about 60% in the initial phase when the primary radicals were generated in a triplet spin state through the photochemical dissociation of C<sub>26</sub>H<sub>27</sub>O<sub>3</sub>P in a relatively high viscosity medium (see Figure 10 (series 10)). However, the effect is very small in the relatively low viscosity medium. The references cited in the introduction explain this effect in terms of the reinforcement of the cage effect due to the reduced mobility of monomers, growing radicals, and solvent molecules in viscous media. Without MF, for the radical pairs initially generated in the T state, spin evolution proceeds in time, passing from the T<sub>0</sub> to the S state and, subsequently, undergoes recombination reactions. In addition, T<sub>+</sub> and T<sub>-</sub> pass to the T<sub>0</sub> state to maintain the condition of equal population of spin states. When MF is applied, the energies for T<sub>+</sub>, T<sub>0</sub> and T<sub>-</sub> splits out. Consequently, primary radicals are generated preferentially in the T<sub>+</sub> state diminishing the possibility for intersystem crossing to T<sub>0</sub> and S states. Therefore, the life-time of the primary radicals is significantly increased with higher probability to escape from the cage. This effect can be interpreted as an increase of  $\Phi$ . Thus, more radicals are released to the medium increasing  $R_p$  and decreasing  $v$ . In low viscosity media the effect is less pronounced. Here, the cage effect is very weak and the time needed for the radicals to escape from the cage may be comparable to the time needed for T<sub>0</sub>–S intersystem crossing. Therefore, approximately the same quantity of radicals is released to the medium independently of their spin states. As a result, very similar  $R_p$  and  $v$  are expected with and without MF.

Interestingly, the augmentation of viscosity due to the formation of polymer molecules in the polymerization medium has no influence on the MF effect. Figure 9 shows no MF increment of  $R_p$  with conversion. Thus, it is speculated that the dimension of molecular cages formed by water, EG and polymer are too small, in the order and too large to trap a C<sub>26</sub>H<sub>27</sub>O<sub>3</sub>P initiator molecule. However, the influences of viscosity induced by molecules of different sizes and its relation with cage dimension and MF effect needs further investigation.

## 5. Conclusions

Polymerization kinetics can be potentially controlled using MF only under very specific reaction conditions. MF effects are significant in systems where primary radical pairs are generated and quenched in a T<sub>+</sub> state. Such radicals are produced by photochemical dissociation of the initiator at relatively low MF intensities and in a viscous reaction medium. The viscosity of the reaction medium must be developed by molecules capable to develop a strong molecular cage over the initiator molecules. The combination of these conditions is critical for the observation of MF effects. MF effects can eventually be interpreted as an increase of  $\Phi$  and a decrease of  $k_t$ . Thus, an increase of  $R_p$  can be expected since both  $\Phi$  and  $k_t$  contribute in the same way. However, the effect on  $v$  would depend on the resulting competition between the increase of  $\Phi$  and the

decrease of  $k_t$ . The modification of the thermal equilibrium of spin states and the molecular orientation induced by MF of 7 Tesla at the temperatures between 308 K and 313 K have negligible effects over the polymerization path.

**Acknowledgments:** The work was supported by the Agencia Nacional de Promoción Científica y Tecnológica, grant PICT 2015 1785 and the Swiss National Science Foundation grants 2000-63395 and 200020-100250. The author thanks Christine Wandrey for her teaching and advice.

**Author Contributions:** I.R. conceived, designed, and performed the experiments, analyzed the data, and wrote the paper.

**Conflicts of Interest:** The author declare no conflict of interest. The founding sponsors had no role in the design of the study; in the collection, analyses, or interpretation of data; in the writing of the manuscript, and in the decision to publish the results.

## References

1. Bhatnagar, S.S.; Mathur, R.N.; Kapur, R.N. The effects of a magnetic field on certain chemical reactions. *Philos. Mag.* **1929**, *8*, 457–473.
2. Selwood, P.W. Magnetism and catalysis. *Chem. Rev.* **1946**, *38*, 41–82.
3. Khudyakov, I.V.; Arsu, N.; Jockusch, S.; Turro, N.J. Magnetic and spin effects in the photoinitiation of polymerization. *Des. Mon. Polym.* **2003**, *6*, 91–101.
4. Bag, D.S.; Maiti, S. Polymerization under magnetic field—II. Radical polymerization of acrylonitrile, styrene and methyl methacrylate. *Polymer* **1998**, *39*, 525–531.
5. Bag, D.S.; Maiti, S. Polymerization under a magnetic field. VI. Triplet dye-sensitized photopolymerization of acrylamide and methyl methacrylate. *J. Polym. Sci. Part A Polym. Chem.* **1998**, *36*, 1509–1513.
6. Chiriac, A.P. Polymerization in magnetic field. XVI. Kinetic aspects regarding methyl methacrylate polymerization in high magnetic field. *J. Polym. Sci. Part A Polym. Chem.* **2004**, *42*, 5678–5686.
7. Chiriac, A.P.; Simionescu, C.I. Some properties of vinyl acetate/methyl methacrylate/acrylamide copolymer synthesized in a magnetic field. *Polym. Test.* **1997**, *16*, 185–192.
8. Chiriac, A.P.; Simionescu, C.I. Aspects regarding the characteristics of some acrylic and methacrylic polyesters synthesized in a magnetic field. *Polym. Test.* **1996**, *15*, 537–548.
9. Huang, J.; Song, Q. Effect of polyethylene glycol with sensitizer groups at both ends on the photoinitiated polymerization of styrene in the water phase in the presence of a magnetic field. *Macromolecules* **1993**, *26*, 1359–1362.
10. Liu, J.; Zhang, R.; Li, H.; Han, B.; Liu, Z.; Jiang, T.; He, J.; Zhang, X.; Yang, G. How does magnetic field affect polymerization in supercritical fluids? Study of radical polymerization in supercritical CO<sub>2</sub>. *New J. Chem.* **2002**, *26*, 958–961.
11. Simionescu, C.I.; Chiriac, A.P.; Chiriac, M.V. Polymerization in a magnetic field: 1. Influence of esteric chain length on the synthesis of various poly(methacrylate)s. *Polymer* **1993**, *34*, 3917–3920.
12. Turro, N.J.; Chow, M.F.; Chung, C.J.; Tung, C.H. An efficient, high conversion photoinduced emulsion polymerization. Magnetic field effects on polymerization efficiency and polymer molecular weight. *J. Am. Chem. Soc.* **1980**, *102*, 7391–7393.
13. Turro, N.J. Application of weak magnetic fields to influence rates and molecular weight distributions of styrene polymerization. *Ind. Eng. Chem. Prod. Res. Dev.* **1983**, *22*, 272–276.
14. Turro, N.J.; Chow, M.F.; Chung, C.J.; Tung, C.H. Magnetic field and magnetic isotope effects on photoinduced emulsion polymerization. *J. Am. Chem. Soc.* **1983**, *105*, 1572–1577.
15. Huang, J.; Hu, Y.; Song, Q. Effect of magnetic field on block copolymerization of styrene and methyl methacrylate by photochemical initiation in micellar solution of poly(ethylene glycol) with sensitizer end group. *Polymer* **1994**, *35*, 1105–1108.
16. Chiriac, A. Polymerization in a magnetic field. 13 Influence of the reaction conditions in the styrene polymerization. *Rev. Roum. Chim.* **2000**, *45*, 689–695.
17. Chiriac, A.P.; Simionescu, C.I. Polymerization in a magnetic field. X. Solvent effect in poly(methyl methacrylate) synthesis. *J. Polym. Sci. Part A Polym. Chem.* **1996**, *34*, 567–573.
18. Keskin, S.; Aydin, M.; Khudyakov, I.; Arsu, N. Study of the polymerization of methyl methacrylate initiated by thioxanthone derivatives: a magnetic field effect. *Turk. J. Chem.* **2009**, *33*, 201–207.

19. Vedenev, A.A.; Khudyakov, I.V.; Golubkova, N.A.; Kuzmin, V.A. External magnetic field effect on the dye-photoinitiated polymerization of acrylamide. *J. Chem. Soc. Faraday Trans.* **1990**, *86*, 3545–3549.
20. Rintoul, I.; Wandrey, C. Magnetic field effects on the copolymerization of water-soluble and ionic monomers. *J. Polym. Sci. Part A Polym. Chem.* **2009**, *47*, 373–383.
21. Rintoul, I.; Wandrey, C. Radical homo- and copolymerization of acrylamide and ionic monomers in weak magnetic field. *Macromol. Symp.* **2008**, *261*, 121–129.
22. Rintoul, I.; Wandrey, C. Magnetic field effects on the free radical solution polymerization of acrylamide. *Polymer* **2007**, *48*, 1903–1914.
23. Odian, G. Radical Chain Polymerization. In *Principles of Polymerization*, 4th ed.; Wiley-Interscience: Hoboken, NJ, USA, 2004; Chapter 3, pp. 198–346.
24. Steiner, U.; Ulrich, T. Magnetic field effects in chemical kinetics and related phenomena. *Chem. Rev.* **1989**, *89*, 51–147.
25. Carrington, A.; McLachlan A.D. *Introduction to Magnetic Resonance, with Applications to Chemistry and Chemical Physics*; Harper International editions: London, UK, 1979.
26. Ayscough, P.B. *Electron Spin Resonance in Chemistry*, Methuen & Co. Ltd.: London, UK, 1967.
27. Sobhi, H.F. Synthesis and Characterization of Acylphosphine Oxide Photoinitiators. Ph.D. Thesis, Cleveland State University, Cleveland, OH, USA, May 2008.
28. Rintoul, I.; Wandrey, C. Limit of applicability of the monomer-enhanced mechanism for radical generation in persulfate initiated polymerization of acrylamide. *Lat. Am. Appl. Res.* **2010**, *40*, 365–372.
29. Rintoul, I.; Wandrey, C. Polymerization of ionic monomers in polar solvents: kinetics and mechanism of the free radical copolymerization of acrylamide/acrylic acid. *Polymer* **2005**, *46*, 4525–4532.
30. Atkins, P.W.; de Paula, J. Statistical thermodynamics. In *Elements of Physical Chemistry*; 6th ed.; Oxford University Press: Oxford, UK, 2013.



© 2017 by the authors; licensee MDPI, Basel, Switzerland. This article is an open access article distributed under the terms and conditions of the Creative Commons by Attribution (CC-BY) license (<http://creativecommons.org/licenses/by/4.0/>).